



POLARITON LUMINESCENCE AND ADDITIONAL BOUNDARY CONDITIONS: COMPARISON BETWEEN THEORY AND EXPERIMENT

Farid Askary and Peter Y. Yu
Department of Physics, University of California
Berkeley, CA 94720

(Received 7 March 1983 by A. A. Maradudin)

Polariton luminescence spectra in semiconductors have been calculated as a function of temperature and impurity trapping rates using a two branch polariton model. Typically, the theoretical spectra show two structures: a peak near the transverse exciton energy and a shoulder near the longitudinal exciton energy. While the lower energy peak is relatively insensitive to the choice of additional boundary conditions (ABC), the higher energy shoulder strongly depends on ABC. The theoretical curves obtained with Pekar's ABC are in quantitative agreement with experimental spectra reported in CdS, CdSe and CuCl. However, significant discrepancies between theory and experiment are found in GaAs and ZnTe.

1. Introduction

Luminescence¹, reflectivity, absorptivity and resonant light scattering measurements^{2,3} in the vicinity of exciton-polaritons in semiconductors have been investigated extensively in the past decade. As a result, polariton luminescence and reflectance spectra are now available for many materials with the zincblende and wurtzite crystal structures. One area of recent interest in polariton physics is the question of the additional boundary condition (ABC)⁴⁻⁷. So far, most investigations of ABC have involved comparison between experimental reflectance spectra and theoretical spectra calculated with different ABC's. There is no theoretical calculation of polariton luminescence spectra including ABC in spite of the existence of many experimental spectra. In this communication we present the first theoretical polariton luminescence spectra obtained with a simple two branch model including the ABC. We demonstrate that the polariton luminescence spectra are sensitive to the ABC adopted and that our simple model with Pekar's ABC can explain quantitatively the experimental spectra in several semiconductors such as CdS, CdSe, and CuCl. Our results indicate that two-branch polariton effects alone are not adequate in explaining the emission spectra in GaAs and ZnTe.

Before presenting our results, we briefly review the present status of experimental and theoretical understanding of polariton luminescence. It is possible to divide the low temperature PL spectra in high quality samples into two types. In semiconductors such as CdS^{8,9}, CdSe and CuCl¹⁰, the PL spectra are dominated by two features: a main peak near the transverse exciton energy E_T , and a shoulder around the longitudinal exciton energy E_L . By contrast, experimental PL spectra in some zincblende type semiconductors such as GaAs¹¹ and ZnTe¹² show two distinct peaks of comparable strength. Although the lower energy peak in these compounds occurs around E_T the higher energy peak usually appears at energies higher than E_L .

It is generally accepted that the lower energy peak near E_T in both cases is due to a maximum in the polariton population. This peak in population is created by a bottleneck effect and was first predicted by Toyozawa¹³. Recently, Sumi¹⁴ has performed a calculation of the PL spectra using a one-branch polariton model and confirmed that the lower energy peak can be accounted for by the polariton bottleneck. However, Sumi's calculation did not show the existence of a higher energy peak or shoulder due to his neglect of the upper polariton branch and the ABC.

Qualitative explanations of the higher energy structure in PL spectra have been proposed. Gross et al.⁸ attributed the higher energy shoulder in CdS PL spectra to an increase in the transmission coefficient of the lower branch polariton near E_L , while Sell et al.¹¹ explained the higher energy peak in GaAs PL spectra as due to emission from the upper polariton branch. Neither hypothesis has yet been tested by quantitative calculations.

2. Model

It is well known that in the vicinity of an exciton resonance in a dielectric the propagating modes of the medium should be coupled transverse exciton and photon modes known as polaritons. In an isotropic medium with a single exciton band the polariton dispersion is given by the following implicit equation¹⁵:

$$\epsilon(k, E) = n^2(k, E) = \frac{\hbar^2 k^2 c^2}{E^2} = \epsilon_b + \frac{4\pi\beta E_T(k)^2}{E_T(k)^2 - E^2} \quad (1)$$

where k and E are respectively the polariton wavevector and energy. ϵ and ϵ_b are respectively the dielectric function and the background dielectric constant without the polariton contribution. n is the index of refraction of polaritons. $4\pi\beta$ and $E_T(k)$ are respectively the oscillator strength and energy of the transverse

exciton. For simplicity we will assume the exciton band to be parabolic with $E_T(k) = E_T(0) + \hbar^2 k^2 / 2m^*$, where m^* is the effective mass of the exciton. The solutions of Eq. 1 lead to two polariton branches as shown in the inset of Fig. 1. The two branches will be referred to as the upper and the lower polariton branches. The longitudinal exciton energy E_L is determined by the condition $\epsilon(0, E=E_L)=0$.

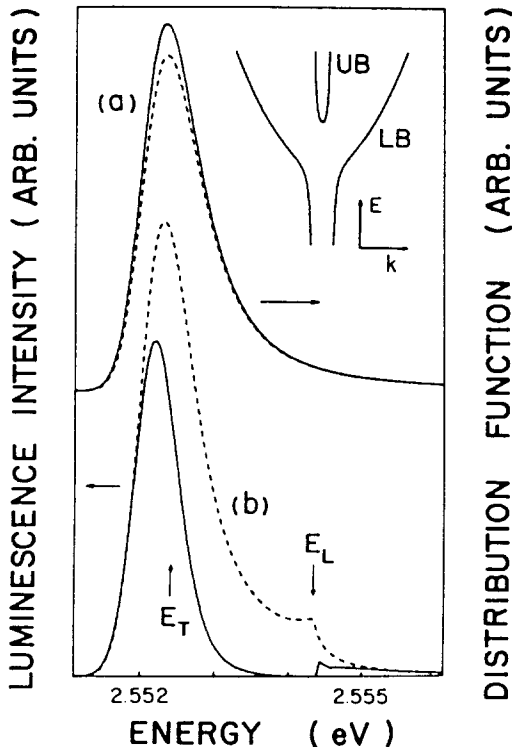


Fig. 1 (a) Distribution function of the lower polariton branch and (b) Luminescence spectra calculated with ABC1 (broken curves) and ABC2 (solid curves). The parameters used are those of CdS as given in Table 1 and are identical for both ABC's. Inset shows a typical polariton dispersion curve.

In the polariton framework, luminescence can be described by the following picture. Incident radiation with energy $\hbar\omega_i > E_L$ is partially transmitted at the sample surface as polaritons. The transmitted polaritons relax via emission of phonons. At the same time some of the polaritons propagate towards the sample surface where they partially escape from the sample and are detected as luminescence photons. As pointed out by Toyozawa¹³ the lower polariton branch has no minimum in energy so, at low temperatures, polaritons do not attain thermal equilibrium among themselves. Under continuous illumination the polariton population will reach a steady state distribution determined by the balance between their rate of

generation and their rate of decay. Sumi¹⁴ performed a numerical calculation based on the above picture by assuming that the polariton has only the lower branch and demonstrated that the population distribution indeed has a peak at an energy close to E_T . However, the PL spectra also depend on the probability that a polariton with a given energy can escape from the sample at the surface i.e., the transmission coefficient of the polariton. In general the calculation of the polariton transmission coefficient requires introduction of additional boundary conditions. Sumi avoided this difficulty by assuming that the polariton has only the lower branch. As a result his calculation does not include any possible contribution of the upper polariton branch to the PL spectra.

The upper polariton branch has, in principle, a twofold effect on the shape of the luminescence spectra. Polariton population in the upper branch can directly contribute to the luminescence via escape from the sample at the surface. Even if this contribution is negligible, the mere presence of the upper branch modifies the transmission coefficient of the lower branch polariton at the sample surface because of the ABC. The latter effect persists at energies below E_L where the upper branch is no longer a propagating mode of the medium⁷.

To explore the effects of the upper polariton branch in PL we have extended Sumi's calculation to include both the upper and the lower polariton branches. The polariton distributions are now given by two coupled Boltzmann equations for ρ_l and ρ_u :

$$\frac{d\rho_l(E)}{dt} = \left(\frac{d\rho_l(E)}{dt} \right)_{in} - \left(\frac{d\rho_l(E)}{dt} \right)_{out} \quad l=l, u \quad (2)$$

where ρ_l and ρ_u are respectively the lower and upper branch polariton distribution functions, $\left(\frac{d\rho_l(E)}{dt} \right)_{in}$ and $\left(\frac{d\rho_l(E)}{dt} \right)_{out}$ represent respectively the rate of generation and the rate of decay of polaritons. To simplify the calculation we assume that the distribution of polaritons is spatially homogeneous in a slab of thickness L , is isotropic in momentum space and is independent of polarization. The latter two assumptions can be justified on the basis that the initial population distribution will be randomized by scattering with phonons.

In the region where the polariton energy E is smaller than E_L the upper branch is not propagating so that the solution of Eq. 2 is essentially the same as that obtained by Sumi; namely,

$$\rho_l(E) = I_l(E) / [P_l(E) + Q_l(E) + R_l(E)] \quad (3)$$

where P is the loss rate due to transmission at the surface and involves the ABC. I , Q , R are respectively the rate of generation due to scattering of polaritons from other states into the state under consideration, loss rate due to scattering with phonons and loss rate due to trapping by impurities. Our expressions for I , Q and R in this energy range are essentially identical to Sumi's. For example, we include only scattering with longitudinal acoustic phonons via the deformation potential interaction.

When $E > E_L$, Eq. 2 involve two coupled equations in ρ_L and ρ_U . The calculation of I and Q can be easily extended to include interbranch scattering. Again, computation of P involves the ABC.

Additional boundary conditions of various forms have been proposed and discussed extensively in the literature⁴⁻⁷. We have considered two such ABC's:

$$\text{ABC1 (Pekar}^4) \quad \sum_i \vec{P}_i = 0 \text{ at the surface} \quad (4)$$

$$\text{ABC2 (Ting et.al.}^5) \quad \sum_i \frac{d\vec{P}_i}{dz} = 0 \text{ at the surface} \quad (5)$$

We note that these two ABC's are special cases of the generalized ABC proposed by Hopfield¹⁶:

$$\alpha \left(\sum_i \vec{P}_i \right) + \beta \left(\sum_i \frac{d\vec{P}_i}{dz} \right) = 0 \quad (6)$$

where α and β are complex quantities in general. Care should be taken in the choice of α and β because some of these choices (such as the so-called soft ABC^{6,7}) may result in ABC's that violate energy conservation¹⁷ and hence will not be considered in this paper.

Finally, we mention some of the limitations of this calculation. In this work, we neglect the possible effects of an exciton-free 'dead layer' on the sample surface. Also, the piezoelectric electron-phonon interaction is not included. Our model is not capable of reproducing the resonant Brillouin spectra largely because we assume that the polariton distribution is isotropic in momentum space.

3. Theoretical Results

As an illustration we present the results obtained by numerical computations under steady state conditions using as input the parameters appropriate for CdS (see Table 1). In Fig. 1(b) we show the PL spectra obtained with both ABC1 and ABC2. The corresponding lower branch polariton distribution functions, $\rho_L(E)$, are shown in Fig. 1(a). The important conclusions we draw from our results for CdS are:

(1) At low temperatures, the contribution of the population of the upper branch to the luminescence is insignificant compared to the luminescence from the population in the lower branch.

(2) The lower branch polariton population shows no structure at $E \sim E_L$ for either ABC1 or ABC2. The higher energy shoulder in the PL spectra depends entirely on the ABC. This shoulder is present for ABC1 but is absent for ABC2.

(3) The lower energy peak in the PL spectra is associated with the peak in the polariton population at the bottleneck and is relatively insensitive to the choice of ABC.

Next, we consider the effects of exciton impurity trapping rate, R , on the shape of the PL spectra calculated with Pekar's ABC. As noted by Sumi, an increase in R tends to quench the population at the bottleneck. In our model, however, this causes the height of the shoulder to increase relative to the main peak.

The effects of temperature on the calculated PL spectra are rather similar. At nonzero

temperatures there is a finite up scattering of polaritons in the bottleneck to the higher energy states. Our calculations show that as temperature increases, the shoulder grows and gradually turns into a small peak. In Fig. 2 we show the effects of relatively large impurity trapping rate and temperature. The apparent shift of the main peak has its origin in the $I_L(E)$ term. The sharp dip in the high temperature spectra is a consequence of neglecting the exciton damping in the polariton dispersion (Eq. 1). Inclusion of a finite exciton damping in the dispersion relation should smooth out this dip.

The combined effects of temperature and impurity trapping rate presumably account for the variation in experimental PL spectra published by different groups on the same material.

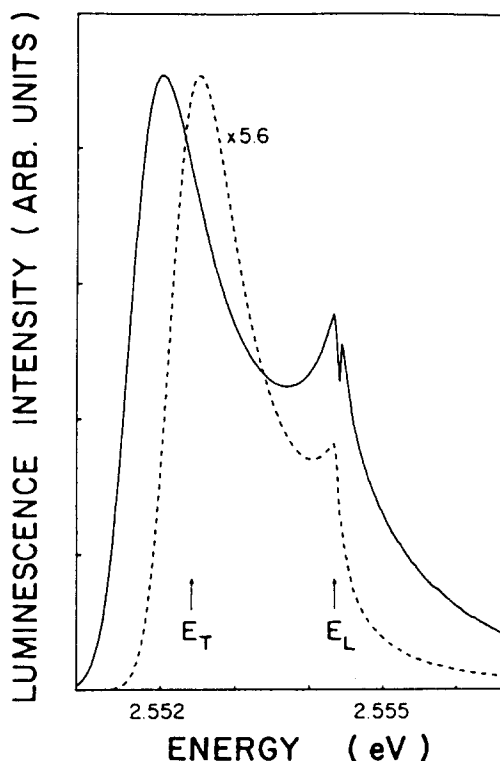


Fig. 2 Luminescence spectra of CdS calculated with Pekar's ABC, solid curve: $T=25$ K, $R=0$; dashed curve: $T=0$ K, $R=8 \times 10^8 \text{ sec}^{-1}$. Other parameters were the same as in Fig. 1.

4. Comparison Between Theory and Experiment

Experimental PL spectra of many semiconductors such as CdS, CuCl and GaAs have been reported by several groups. In addition, we have obtained extensive low temperature luminescence and reflectivity spectra of CdS, CdSe and GaAs in our laboratory. Our best spectra resemble those published in the literature. We believe that the experimental PL spectra of these four materials: CdS (Ref.8), CdSe, CuCl (Ref.10), and GaAs as shown in Fig. 3 (a)-(d) represent reliable and reproducible PL spectra. A few words about CdSe spectrum are, however, in order.

Table 1

Parameters used in the calculation of PL spectra of Fig. 3

Parameter	Definition	Units	CdS	CdSe	CuCl	GaAs
E_T	Transverse exciton energy	(eV)	2.5524 ^{a,b}	1.8227 ^{a,c}	3.2019 ^{a,d}	
E_L	Longitudinal Exciton energy	(eV)				1.5151 ^e
ΔE_{LT}	Longitudinal-transverse splitting	(meV)	1.92 ^f	1.86 ^g	5.5 ^h	0.08 ⁱ
ϵ_b	Background dielectric constant		9.1 ^j	8.4 ^k	4.66 ^l	12.56 ⁱ
m^*	Exciton effective mass	(m_e)	0.94 ^j	0.58 ^m	2.3 ^l	0.6 ⁱ
u	Velocity of sound longitudinal	(10^5 cm/sec)	4.4 ⁿ	3.57 ^o	3.8 ^p	4.8 ⁱ
ρ	Density	(g/cm ³)	4.82 ⁿ	5.66	4.155 ^p	5.307 ^q
D	Exciton deformation potential	(eV)	2.5 ⁿ	2 ^r	1.2 ^s	7.8 ^q
R	Exciton impurity trapping rate	(10^9 sec ⁻¹)	0.4 ^p	0.1 ^p	3.6 ^p	0
T	Temperature	(K)	0	0	0	5
L	Thickness of the Slab	(μ)	1	1	1	1
θ	Angle of observation outside the crystal	(degrees)	35	35	35	35

a) Adjusted slightly for optimum fit to the experimental spectra.

b) Value quoted by Gross et. al.⁸ is 2.5525 eV.c) 0.3 meV less than the peak in E_{llc} spectra.d) 0.3 meV less than the value quoted in ⁴.

e) Accurately determined from reflectivity spectra. (See text and also Ref. 11, and 1).

f) Ref. 3, p. 101.

g) Chosen for best fit. See text.

h) Y. Masumoto, Y. Usuma and S. Shionoya, Proc. 15th Internat. Conf. Phys. Semicond. Kyoto, 1980. J. Phys. Soc. Japan 49 (1980) Suppl. A, p. 393.

i) R. G. Ulbrich and C. Weisbuch, Phys. Rev. Lett. 38, 865 (1977) and Ref. 2, p. 233.

j) P.Y. Yu and F. Evangelisti, Phys. Rev. Lett. 42, 1642 (1979).

k) Ref. 18

l) Y. Segawa, Y. Aoyagi and S. Namba, Solid State Commun. 39, 535 (1981)

m) R.G. Wheeler and J.O. Dimmock, Phys. Rev. 125, 1805 (1962) and Ref. 19

n) Ref. 14

o) V.A. Kiselev, B.S. Razbirin and I.N. Uraltsev, Phys. Stat. Sol. (6) 72, 161 (1975).

p) T.H.K. Barron, J.A. Birch and G.K. White, J. Phys. C10, 1617 (1977).

q) N. Neuberger, III-V Semiconducting Compounds, Handbook of Electronic Materials v.2, (Plenum 1971) p. 45 & 53.

r) M. Grynberg, Phys. Stat. Sol. 27, 255 (1968), Averaged over llc and lc .

s) T. Koda, T. Murahashi, T. Mitani, S. Sokoda and Y. Onodera, Phys. Rev. B 5, 705 (1972).

t) Adjustable parameter of the calculation. See text. The large value for CuCl is indicative of a relatively impure sample.

Although the PL and reflectivity spectra of various CdSe samples we have measured are qualitatively similar, the energy of the longitudinal exciton, as determined from reflectivity measurements, varies by as much as 5 meV. The variations in the longitudinal-transverse energy splitting ΔE_{LT} are even more drastic. Values ranging from 0.5 to 1.3 meV have been reported by different authors¹⁸⁻²¹. Similar large variations have been observed by us. At the moment we do not understand this large sample to sample variation in ΔE_{LT} which seems to be particular to

CdSe. As a result, we have treated ΔE_{LT} of CdSe as an adjustable parameter. Otherwise the theoretical spectra in Fig. 3 (broken curves) have all been obtained with polariton parameters (listed in Table 1) measured independently by other techniques. The only exception is the impurity scattering rate R which cannot be yet determined by an independent technique. In Figs. 3(a) and (b) the bound exciton backgrounds have been approximated by Lorentzians shown as dotted-dashed curves.

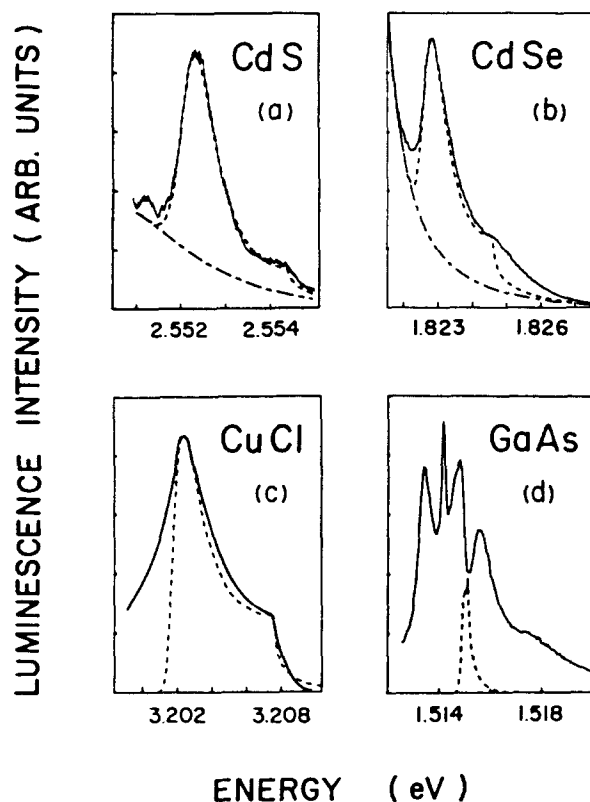


Fig. 3 Comparison between theoretical and experimental PL spectra for (a) CdS (b) CdSe (c) CuCl and (d) GaAs (solid curves: experimental spectra; dashed curves: theoretical spectra; dashed-dotted curves: bound exciton background). The parameters for the theoretical spectra are given in Table 1. The theoretical curve in (a) is the same curve in Fig. 1(b) but now superimposed on a Lorentzian background due to bound excitons.

Overall, we find that ABC1 produces theoretical PL spectra in much better agreement with experimental spectra than ABC2. Since we have not investigated other ABC's, we cannot conclude that ABC1 is the correct ABC to use. Among the four semiconductors we show in Fig. 3 our model

produces quantitative agreement with experiment for CdS, CdSe and CuCl. Although we have not performed detailed calculations for other materials, we believe that our model with Pekar's ABC can also explain the PL spectra of CdTe²², CuI¹, and CuBr¹. However, qualitative discrepancies exist between experimental PL spectra and the predictions of our model for GaAs. The two experimentally observed peaks at 1.5148 and 1.5155 eV in Fig. 3(d) have been attributed (by Sell et al.¹¹) respectively to luminescence from the lower and the upper polariton branches. With our model we found two closely spaced structures near 1.5151 eV where the experimental spectrum showed a dip. One may be tempted to adjust E_L in order to line up these structures with one of the peaks in the experimental spectrum. However, this will make the interpretation of the PL spectrum inconsistent with the reflectivity spectrum on the same sample since E_L can be determined very precisely from the sharp spike in the reflectivity spectrum¹¹. A more detailed discussion of the discrepancies between experiment and theory in GaAs will be deferred to a future publication. For now it suffices to state that we have not been able to explain even qualitatively the polariton emission spectra in GaAs by modifying our model to include additional effects such as an exciton-free 'dead' layer. We also note that similar discrepancies between theory and experiment seem to exist for ZnTe¹². Finally, we should point out that alternative explanations for the luminescence spectra in GaAs have been proposed²³. In view of our calculation such alternative models have to be seriously considered.

In conclusion we have presented a numerical calculation of polariton luminescence lineshape based on a simple two branch polariton model including the ABC. We demonstrate that the PL lineshape, especially the magnitude of the higher energy shoulder around E_L , is sensitive to the ABC. We found that our model with the Pekar's ABC explains satisfactorily the general behavior of PL spectra in CdS, CdSe, and CuCl. However, in GaAs and ZnTe our model cannot account for the peak which appears above E_L in these materials.

We are grateful to the following people for generously providing us with samples: H. Cummins, D. Reynolds, Y. Petroff and C. Liechti. Helpful discussions with N. Caswell are also acknowledged. This work was supported by a grant from NSF No. DMR 79-19463.

References

1. S. Suga, K. Cho, P. Hiesinger and T. Koda, J. Lum. **12/13**, 109 (1976).
2. C. Weisbuch and R.G. Ulbrich in "Light Scattering in Solids III" edited by M. Cardona and G. Guntherodt (Springer-Verlag, 1982) Ch. 7.
3. E.S. Koteles in "Exciton" edited by E.I. Rashba and M.D. Sturge (North-Holland Publishing Co., 1982) Ch. 3.
4. S. I. Pekar, Zh. Eksperim. i. Teor. Fiz. **33**, 1022 (1957); **34**, 1176 (1958) [Sov. Phys. JETP **6**, 785 (1958); **7**, 813 (1958)].
5. C.S. Ting, M.J. Frankel and J.L. Birman, Solid State Commun. **17**, 1285 (1975).
6. G.S. Agarwal, D.N. Pattanayak and E. Wolf, Opt. Commun. **4**, 225 (1971); **4**, 260 (1971).
7. A.A. Maradudin and D.L. Mills, Phys. Rev. B **7**, 2787 (1973).
8. E. Gross, S. Permogorov, V. Travnikov and A. Selkin, Solid State Commun. **10**, 1071 (1972).
9. P. Wiesner and U. Heim, Phys. Rev. B **11**, 3071 (1975).
10. S. Suga and T. Koda, Phys. Stat. Sol. (b) **66**, 255 (1974).
11. S.E. Stokowski, D.D. Sell and J.V. DiLorenzo, Phys. Rev. B **7**, 4568 (1973).

12. M.S. Brodin and M.G. Matsko, *Solid State Commun.* 35, 375 (1980).
13. Y. Toyozawa, *Progr. Theor. Phys. Suppl.* 12, 111 (1959).
14. H. Sumi, *J. Phys. Soc. Japan* 41, 526 (1976).
15. J.J. Hopfield, *Phys. Rev.* 112, 1555 (1958).
16. J.J. Hopfield and D. G. Thomas, *Phys. Rev.* 132, 563 (1963).
17. M.F. Bishop and A.A. Maradudin, *Phys. Rev. B* 14, 3384 (1976).
18. C. Hermann and P.Y. Yu, *Solid State Commun.* 28, 313 (1978).
19. V.A. Kiselev, B.S. Razbirin and I.N. Uraltsev, "Proceedings of the XII International Conference on the Physics of Semiconductors", ed. by M.A. Pilkuhn (B.G. Teubner, Stuttgart, 1974) p. 996.
20. R. Planel, M. Nawrochi and C. Benoit à la Guillaume, *Nuovo Cimento* 39B, 519 (1977).
21. T. Itoh, P. Lavallard, J. Reydellet and C. Benoit à la Guillaume, *Solid State Commun.* 37, 925 (1981).
22. Le Si Dung, G. Neu and R. Romestain, *Solid State Commun.* 44, 1187 (1982).
23. K. Aoki, T. Kinugasa and K. Yamamoto, *Phys. Lett.* 72A, 63 (1979).